

# Extraction of GPDs from DVCS off unpolarized target

**Krešimir Kumerički**

Physics Department  
University of Zagreb, Croatia

Collaboration with:

Dieter Müller (Bochum, Berkeley),  
Andreas Schäfer (Regensburg)

*GPD2010 workshop: "Hard Meson and Photon Electroproduction"*

11-15 Oct 2010, ECT\*, Trento

# Outline

DVCS - introduction

The model

Global fit results

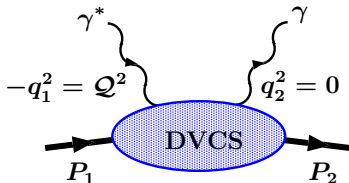
Predictions for future experiments

Neural nets approach

## Probing the proton with two photons

- Deeply virtual Compton scattering (DVCS) [Müller '92, et al. '94]

$$t = (P_2 - P_1)^2, \quad q = (q_1 + q_2)/2$$



Generalized Bjorken limit:

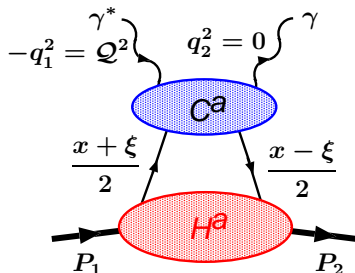
$$-q^2 \simeq Q^2/2 \rightarrow \infty$$

$$\xi = \frac{-q^2}{2P \cdot q} \rightarrow \text{const}$$

- To twist-two accuracy (and neglecting gluon transversity) cross-section can be expressed in terms of four **Compton form factors** (CFF)

$$\mathcal{H}(\xi, t, Q^2), \quad \mathcal{E}(\xi, t, Q^2), \quad \tilde{\mathcal{H}}(\xi, t, Q^2), \quad \tilde{\mathcal{E}}(\xi, t, Q^2).$$

# Factorization of CFFs $\longrightarrow$ GPDs



- Compton form factor is a convolution:

$${}^a\mathcal{H}(\xi, t, Q^2) = \int dx C^a(x, \xi, Q^2/\mu^2) H^a(x, \eta = \xi, t, \mu^2)$$

$$a = \text{NS}, S(\Sigma, G)$$

- $H^a(x, \eta, t, \mu^2)$  — Generalized parton distribution (GPD)

## Model-dependent extraction of GPDs

$$^a\mathcal{H}(\xi, t, Q^2) = \int dx C^a(x, \xi, Q^2/\mu^2) H^a(x, \eta = \xi, t, \mu^2)$$

- convolution is not generally invertible so we can extract GPDs only by modelling them and comparing to experiment

Our present model (details on the next few slides):

- We model **sea quark and gluon GPDs** in conformal moment space, we expand them in  $t$ -channel  $SO(3)$  partial waves, and take into account LO QCD evolution.
- We model **valence quark GPDs** by parametrizing them on  $\eta = x$  trajectory, which at LO gives  $\Im m\mathcal{H}$  directly, and  $\Re e\mathcal{H}$  via dispersion relations. Here we ignore evolution which is probably negligible in kinematic region where valence quarks are not.

## Modelling GPDs in moment space

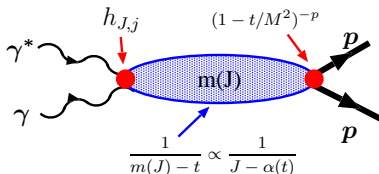
- Instead of considering momentum fraction dependence  $H(\mathbf{x}, \dots)$
- ... it is convenient to make a transform into complementary space of **conformal moments**  $j$ :

$$H_j^q(\eta, \dots) \equiv \frac{\Gamma(3/2)\Gamma(j+1)}{2^{j+1}\Gamma(j+3/2)} \int_{-1}^1 dx \eta^j C_j^{3/2}(x/\eta) H^q(\mathbf{x}, \eta, \dots)$$

- $H_j$  do not mix under evolution at LO
- Measurable on the lattice [M. Goeckeler's talk]
- For integer  $j$ , they are even polynomials in  $\eta$
- In our case, they are continued to complex  $j$  to allow OPE series summation

## Modelling conformal moments of GPDs

- $H_j(t)$  are modelled by SO(3) partial wave decomposition of  $t$ -channel  $\gamma^*\gamma$  scattering

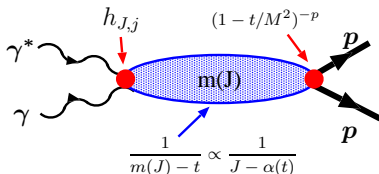


$$H_j(\eta, t) = \sum_J^{j+1} h_{J,j} \frac{1}{J - \alpha(t)} \frac{1}{\left(1 - \frac{t}{M^2(J)}\right)^p} \eta^{j+1-J} d_{0,\nu}^J(\eta)$$

- $d_{0,\nu}^J(\eta)$  — Wigner SO(3) functions (Legendre, Gegenbauer, ...)

## Modelling conformal moments of GPDs

- $H_j(t)$  are modelled by SO(3) partial wave decomposition of  $t$ -channel  $\gamma^*\gamma$  scattering



$$H_j(\eta, t) = \sum_J^{j+1} h_{J,j} \frac{1}{J - \alpha(t)} \frac{1}{\left(1 - \frac{t}{M^2(J)}\right)^p} \eta^{j+1-J} d_{0,\nu}^J(\eta)$$

- $d_{0,\nu}^J(\eta)$  — Wigner SO(3) functions (Legendre, Gegenbauer, ...)
- Similar to “dual” parametrization [Polyakov, Shuvaev '02; K. Semenov's talk]



## Leading partial wave (PW) model

- Taking just a leading partial wave  $J = j + 1$  gives ansatz:

$$\mathbf{H}_j(\eta, t, \mu_0^2) = \begin{pmatrix} N'_\Sigma F_\Sigma(t) B(1 + j - \alpha_\Sigma(0), 8) \\ N'_G F_G(t) B(1 + j - \alpha_G(0), 6) \end{pmatrix}$$

$$\alpha_a(t) = \alpha_a(0) + 0.15t \quad F_a(t) = \frac{j + 1 - \alpha(0)}{j + 1 - \alpha(t)} \left(1 - \frac{t}{M_0^2}\right)^{-p_a}$$

... corresponding in forward case to **PDFs** of form

$$\Sigma(x) = N'_\Sigma x^{-\alpha_\Sigma(0)} (1 - x)^7; \quad G(x) = N'_G x^{-\alpha_G(0)} (1 - x)^5$$

## Leading partial wave (PW) model

- Taking just a leading partial wave  $J = j + 1$  gives ansatz:

$$\mathbf{H}_j(\eta, t, \mu_0^2) = \begin{pmatrix} N'_\Sigma F_\Sigma(t) B(1+j-\alpha_\Sigma(0), 8) \\ N'_G F_G(t) B(1+j-\alpha_G(0), 6) \end{pmatrix}$$

$$\alpha_a(t) = \alpha_a(0) + 0.15t \quad F_a(t) = \frac{j+1-\alpha(0)}{j+1-\alpha(t)} \left(1 - \frac{t}{M_0^2}\right)^{-p_a}$$

... corresponding in forward case to **PDFs** of form

$$\Sigma(x) = N'_\Sigma x^{-\alpha_\Sigma(0)} (1-x)^7; \quad G(x) = N'_G x^{-\alpha_G(0)} (1-x)^5$$

- $M_0^G = \sqrt{0.7} \text{ GeV}$  is fixed by the  $J/\psi$  production data
- Single free parameter:  $M_0^\Sigma$  (after DIS  $F_2$  fit fixes the rest)

For small  $\xi$  (small  $x_{Bj}$ ) valence quarks are less important  $\Rightarrow \Sigma \approx \text{sea}$

## Subleading PW — flexible models

$$\mathbf{H}_j(\eta, t) = \underbrace{\left( \begin{array}{c} N'_{\text{sea}} F_{\text{sea}}(t) B(1+j-\alpha_{\text{sea}}(0), 8) \\ N'_G F_G(t) B(1+j-\alpha_G(0), 6) \end{array} \right)}_{\text{skewness } r \approx 1.6 \text{ (too large)}} + \underbrace{\left( \begin{array}{c} \text{(subleading par-} \\ \text{tial waves, } \eta\text{-} \\ \text{dependence!} \end{array} \right)}_{< 0}$$

negative skewness

- **Leading PW model:** works only at (N)NLO [K.K., D. Müller and K. Passek-Kumerički '07]
- **Leading and second PW:** LO fits are fine, but gluon  $H^G(x, x, t)$  tends to be negative for small  $x$  [K.K. and D. Müller '08]
- **Adding third PW:** everything fine [K.K. and D. Müller '10]
- Strengths of second and third quark and gluon partial wave are **4 additional model parameters.**

## Modelling valence GPDs

- Neglecting evolution allows a simple model of GPDs on  $\eta = x$  trajectory:

$$H^{\text{val}}(x, x, t) = 1.35 r \left( \frac{2x}{1+x} \right)^{-\alpha(t)} \left( \frac{1-x}{1+x} \right)^b \frac{1}{\left( 1 - \frac{1-x}{1+x} \frac{t}{M^2} \right)},$$

$$\tilde{H}^{\text{val}}(x, x, t) = 0.6 \tilde{r} \left( \frac{2x}{1+x} \right)^{-\alpha(t)} \left( \frac{1-x}{1+x} \right)^{\tilde{b}} \frac{1}{\left( 1 - \frac{1-x}{1+x} \frac{t}{\tilde{M}^2} \right)}.$$

- $\alpha(t) = 0.43 + 0.85 t/\text{GeV}^2$  from  $(\rho, \omega)$  Regge trajectories; non-Regge  $t$ -dependence taken from spectator model [Hwang, Müller '07]
- Six free parameters:  $r, b, M, \tilde{r}, \tilde{b}, \tilde{M}$
- GPD  $E$  kinematically suppressed and neglected
- GPD  $\tilde{E}$  modelled by pion pole contribution (2 parameters)

## Usage of dispersion relations

[Teryaev '05; K.K., Müller and Passek-K. '07, '08; Diehl and Ivanov '07]

- LO perturbative prediction is “handbag” amplitude

$$\mathcal{H}(\xi, t, Q^2) \stackrel{\text{LO}}{=} \int_{-1}^1 dx \left( \frac{1}{\xi - x - i\epsilon} - \frac{1}{\xi + x - i\epsilon} \right) H(x, \xi, t, Q^2)$$

- giving access to GPD on the “cross-over” line  $\eta = x$

$$\frac{1}{\pi} \Im \mathcal{H}(\xi = x, t, Q^2) \stackrel{\text{LO}}{=} H(x, x, t, Q^2) - H(-x, x, t, Q^2)$$

- while dispersion relation connects it to  $\Re \mathcal{H}$  and at the most one subtraction constant  $\mathcal{C}_{\mathcal{H}} = -\mathcal{C}_{\mathcal{E}}$ ;  $\mathcal{C}_{\tilde{\mathcal{H}}} = \mathcal{C}_{\tilde{\mathcal{E}}} = 0$

$$\Re \mathcal{H}(\xi, t, Q^2) = \frac{1}{\pi} \text{PV} \int_0^1 d\xi' \left( \frac{1}{\xi - \xi'} - \frac{1}{\xi + \xi'} \right) \Im \mathcal{H}(\xi', t, Q^2) + \underbrace{\frac{\mathcal{C}}{(1 - t/M_C^2)^2}}_{\mathcal{C}_{\mathcal{H}}(t, Q^2)}$$

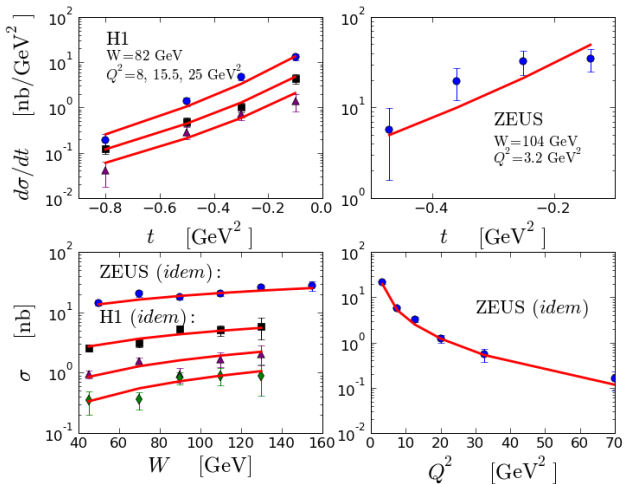
## Example fit result (preliminary)

- experimental data organized in standardized computer- and human-readable files
- Expressions for observables from [Belitsky, Müller and Kirchner '01, Belitsky and Müller '10]
- MINUIT minimizing routine [James and Roos '75]
- 15 parameter fit to 175 experimental points:  $\chi^2/d.o.f = 132/160$

```
-----  
M02S = 0.51 +- 0.02  
SECS = 0.28 +- 0.02  
SECG = -2.79 +- 0.12  
THIS = -0.13 +- 0.01  
THIG = 0.90 +- 0.05  
  Mv = 4.00 +- 3.33 (edge)  
  rv = 0.62 +- 0.06  
  bv = 0.40 +- 0.67  
  C = 8.78 +- 0.98  
  MC = 0.97 +- 0.11  
tMv = 0.88 +- 0.24  
trv = 7.76 +- 1.39  
tbv = 2.05 +- 0.40  
rpi = 3.54 +- 1.77  
Mpi = 0.73 +- 0.37  
-----
```

# H1 (2007), ZEUS (2008)

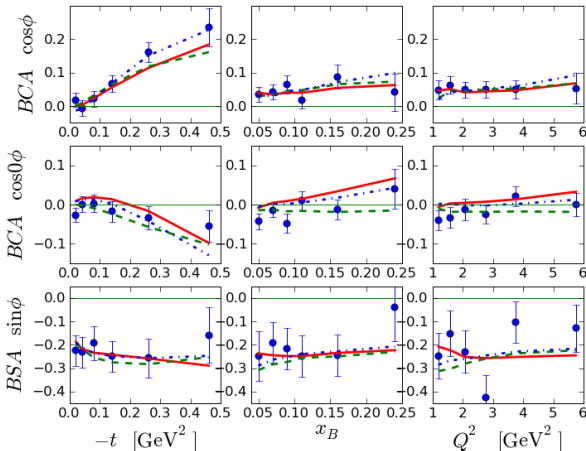
- 107 measurements of  $\sigma^{\text{DVCS}}$  and  $d\sigma^{\text{DVCS}}/dt \sim |\mathcal{H}|^2$



## HERMES (2008)

(18 points)  $BCA \equiv \frac{d\sigma_{e^+} - d\sigma_{e^-}}{d\sigma_{e^+} + d\sigma_{e^-}} \sim A_C^{\cos 0\phi} + A_C^{\cos 1\phi} \cos \phi \sim \Re \mathcal{H}$

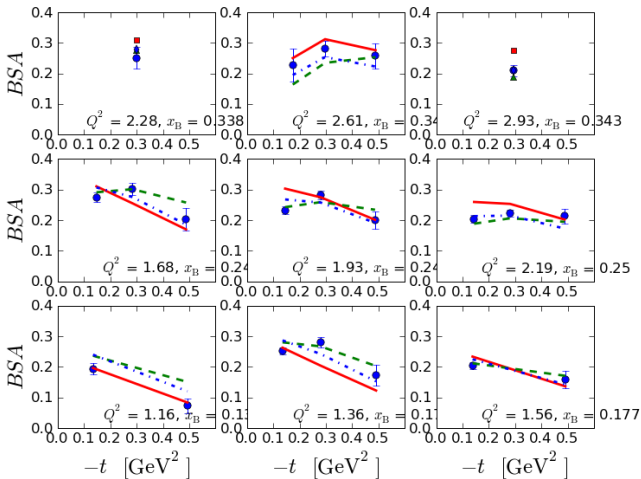
(18 points)  $BSA \equiv \frac{d\sigma_{e^\uparrow} - d\sigma_{e^\downarrow}}{d\sigma_{e^\uparrow} + d\sigma_{e^\downarrow}} \sim A_{LU}^{\sin 1\phi} \sin \phi \sim \Im m \mathcal{H}$





## CLAS (2007)

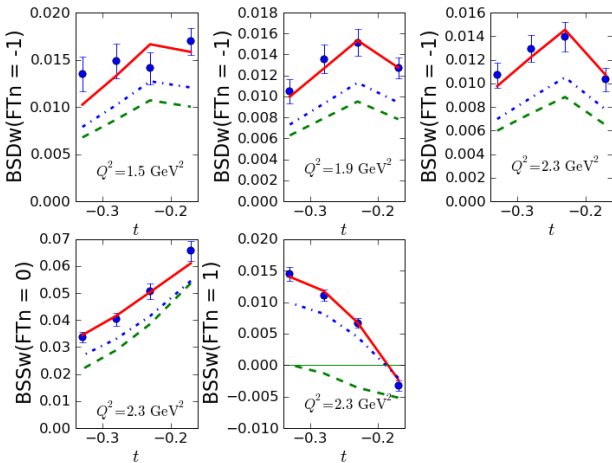
- (12 points,  $|t| \leq 0.3 \text{ GeV}^2$ )  $\sin\phi$  harmonics of BSA



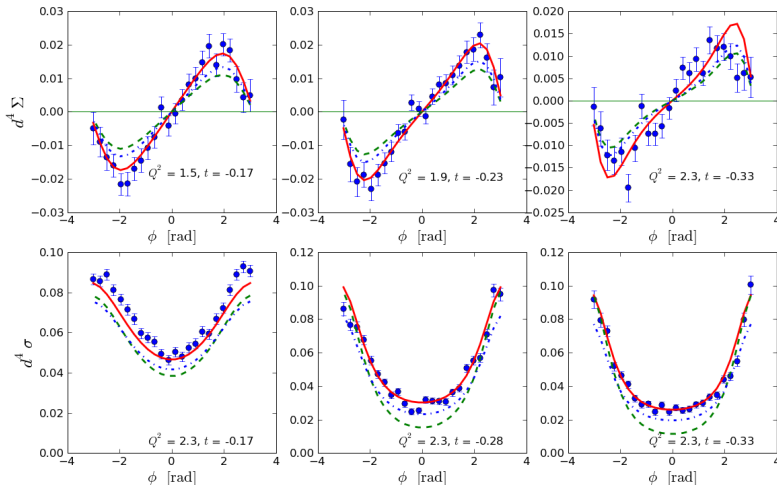
- Some outliers here?!

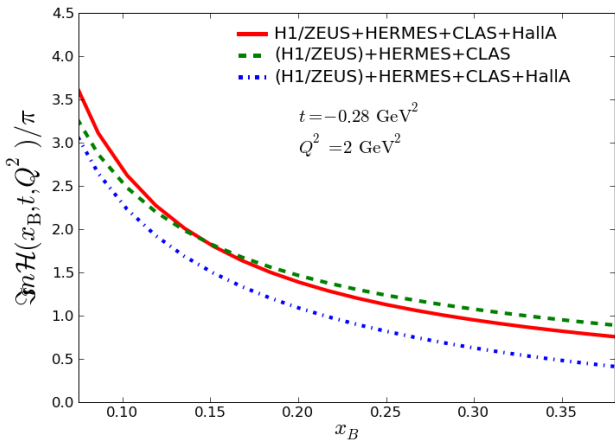
# HALL A (2006) — harmonics

- (12 pts)  $\text{BSD} = d\sigma_{e\uparrow} - d\sigma_{e\downarrow}$   $\sin\phi$  harmonic
- (8 pts)  $\text{BSS} = d\sigma_{e\uparrow} + d\sigma_{e\downarrow}$   $\cos 0\phi$  and  $\cos\phi$  harmonics
- Fit is OK only with unusually large  $\Re\mathcal{T}_{\text{DVCS}}$  ( $\rightarrow \tilde{\mathcal{H}}, \tilde{\mathcal{E}}$ )



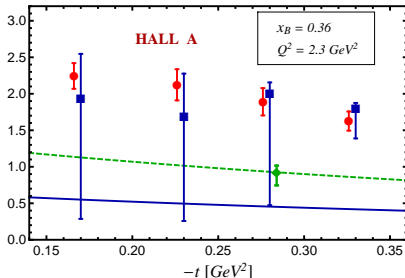
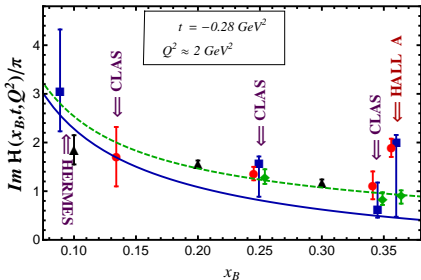
# HALL A (2006) — $\phi$ -dependence

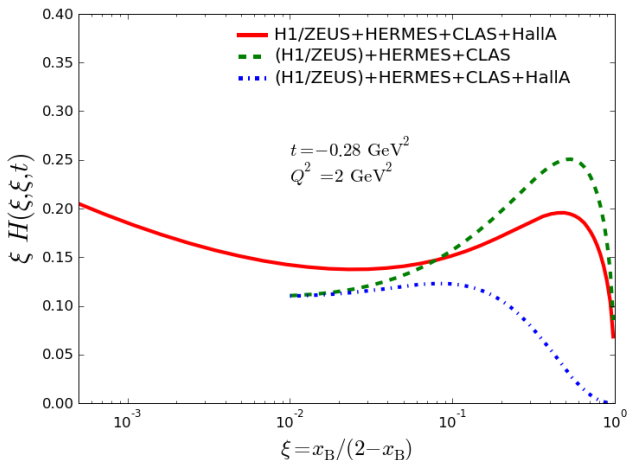


Resulting  $\Im m\mathcal{H}(x_B, t, Q^2)$ 

# Comparison to other fitting approaches

- We have rough agreement with other fitting approaches (dual-model fit [Moutarde '09], model-independent fits: [Guidal '08], [Guidal and Moutarde '09]), although there are some discrepancies for Hall A data



Resulting  $H(x, x, t)$ 

- Shape of GPD at very large- $x$  still very unknown, but predictions for COMPASS/EIC/JLAB@12 are possible

# H1 beam charge asymmetry

$$BCA \equiv \frac{d\sigma_{e^+} - d\sigma_{e^-}}{d\sigma_{e^+} + d\sigma_{e^-}} = \frac{\mathcal{A}_{\text{Interference}}}{|\mathcal{A}_{\text{DVCS}}|^2 + |\mathcal{A}_{\text{BH}}|^2} \stackrel{\text{LO}}{\propto} F_1 \text{Re}\mathcal{H} + \frac{|t|}{4M^2} F_2 \text{Re}\mathcal{E}$$

# H1 beam charge asymmetry

$$BCA \equiv \frac{d\sigma_{e^+} - d\sigma_{e^-}}{d\sigma_{e^+} + d\sigma_{e^-}} = \frac{\mathcal{A}_{\text{Interference}}}{|\mathcal{A}_{\text{DVCS}}|^2 + |\mathcal{A}_{\text{BH}}|^2} \stackrel{\text{LO}}{\propto} F_1 \text{Re}\mathcal{H} + \frac{|t|}{4M^2} F_2 \text{Re}\mathcal{E}$$

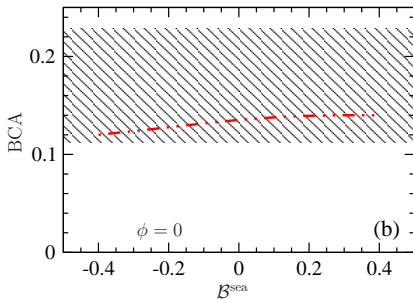
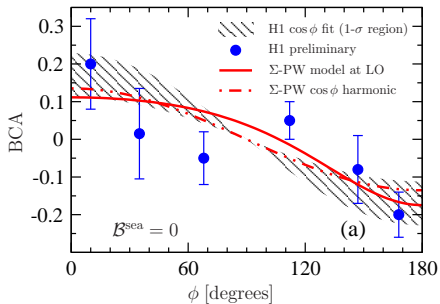
- Model  $E_{\text{sea}}$  as  $(\mathcal{B}_{\text{sea}}/N_{\text{sea}})H_{\text{sea}}$  and take  $\mathcal{B}_{\text{sea}} \equiv \int dx x E_{\text{sea}}$  as a parameter



# H1 beam charge asymmetry

$$BCA \equiv \frac{d\sigma_{e^+} - d\sigma_{e^-}}{d\sigma_{e^+} + d\sigma_{e^-}} = \frac{\mathcal{A}_{\text{Interference}}}{|\mathcal{A}_{\text{DVCS}}|^2 + |\mathcal{A}_{\text{BH}}|^2} \stackrel{\text{LO}}{\propto} F_1 \text{Re}\mathcal{H} + \frac{|t|}{4M^2} F_2 \text{Re}\mathcal{E}$$

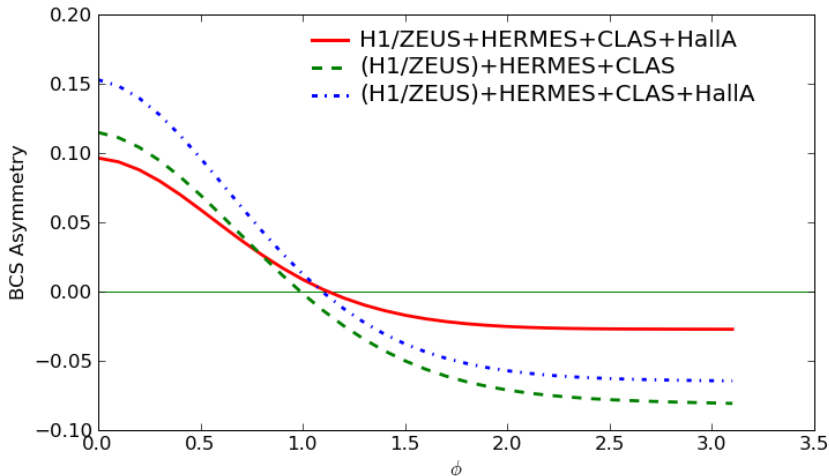
- Model  $E_{\text{sea}}$  as  $(\mathcal{B}_{\text{sea}}/N_{\text{sea}})H_{\text{sea}}$  and take  $\mathcal{B}_{\text{sea}} \equiv \int dx x E_{\text{sea}}$  as a parameter



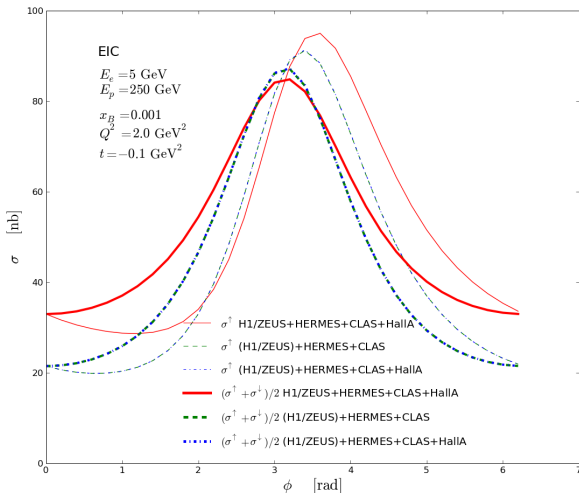
- We cannot extract  $\mathcal{B}_{\text{sea}}$  from H1 data

# Prediction for COMPASS beam charge-spin asymmetry

$$A_{\text{BCSA}}(\phi) = \frac{d\sigma^{\uparrow+} - d\sigma^{\downarrow-}}{d^{\uparrow+\sigma} + d^{\downarrow-\sigma}}$$



# Prediction for EIC cross section



## Problems with standard fitting approaches

1. Choice of fitting function introduces theoretical bias leading to systematic error which cannot be estimated
2. Propagation of uncertainties from experiment to fitted function is difficult. (Correlations are usually lost.)

## Fitting with neural networks

1. Neural networks make bias-free interpolation of data
2. Training networks on Monte Carlo replicated data preserves experimental uncertainties and their correlations [Giele et al. '01]

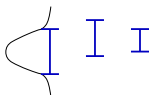
## Fitting with neural networks

1. Neural networks make bias-free interpolation of data
2. Training networks on Monte Carlo replicated data preserves experimental uncertainties and their correlations [Giele et al. '01]



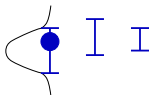
## Fitting with neural networks

1. Neural networks make bias-free interpolation of data
2. Training networks on Monte Carlo replicated data preserves experimental uncertainties and their correlations [Giele et al. '01]



## Fitting with neural networks

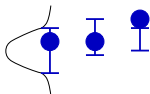
1. Neural networks make bias-free interpolation of data
2. Training networks on Monte Carlo replicated data preserves experimental uncertainties and their correlations [Giele et al. '01]





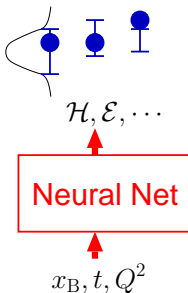
## Fitting with neural networks

1. Neural networks make bias-free interpolation of data
2. Training networks on Monte Carlo replicated data preserves experimental uncertainties and their correlations [Giele et al. '01]



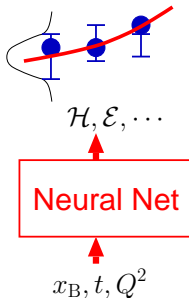
## Fitting with neural networks

1. Neural networks make bias-free interpolation of data
2. Training networks on Monte Carlo replicated data preserves experimental uncertainties and their correlations [Giele et al. '01]



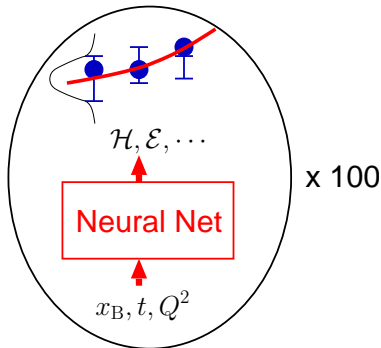
## Fitting with neural networks

1. Neural networks make bias-free interpolation of data
2. Training networks on Monte Carlo replicated data preserves experimental uncertainties and their correlations [Giele et al. '01]



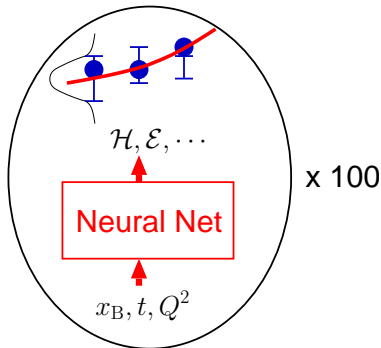
## Fitting with neural networks

1. Neural networks make bias-free interpolation of data
2. Training networks on Monte Carlo replicated data preserves experimental uncertainties and their correlations [Giele et al. '01]



## Fitting with neural networks

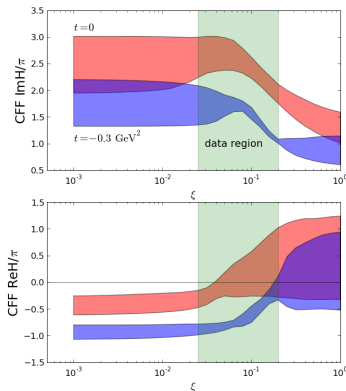
1. Neural networks make bias-free interpolation of data
2. Training networks on Monte Carlo replicated data preserves experimental uncertainties and their correlations [Giele et al. '01]



- Already successfully applied to PDF fitting by [NNPDF] group. Has maybe even larger potential in GPD fitting with GPD being less-known function of more variables.

## Sample result (preliminary)

- 78 neural nets with neuron architecture 2-16-12-2 trained on CLAS BSA and HERMES BCA



Error bands unreliable at the moment!

- There are other interesting machine-learning approaches to parton structure [S. Liuti et al.]

## Summary

- Global fits to unpolarized target H1, ZEUS, HERMES and CLAS data are possible within assumption of GPD  $H$  dominance
- cross sections measured by Hall A require additional contributions ( $\tilde{H}$  or  $\tilde{E}$ ).
- **For the future:** Inclusion of data on DVCS with polarized target, and on meson production [T. Lautenschlager, K. Passek-Kumerički, et al. work in progress].

## Summary

- Global fits to unpolarized target H1, ZEUS, HERMES and CLAS data are possible within assumption of GPD  $H$  dominance
- cross sections measured by Hall A require additional contributions ( $\tilde{H}$  or  $\tilde{E}$ ).
- **For the future:** Inclusion of data on DVCS with polarized target, and on meson production [T. Lautenschlager, K. Passek-Kumerički, et al. work in progress].

The End



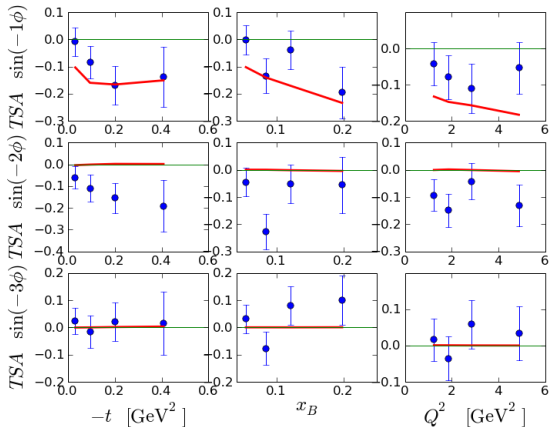
- Probability  $P(\chi^2/d.o.f.)$  and parameter values

[unpolarized target] H1ZEUS+UNP5 P(131.94, 160) = 0.95	[unp. + pol. target] H1ZEUS+UNP5+TSA1 P(196.41, 172) = 0.1	[unp. + pol. target] H1ZEUS+UNP5+TSA1 (Q2min=1.6) P(168.82, 156) = 0.23
M02S = 0.51 +- 0.02	M02S = 0.54 +- 0.02	M02S = 0.52 +- 0.02
SECS = 0.28 +- 0.02	SECS = 1.49 +- 0.02	SECS = 0.57 +- 0.03
THIS = -0.13 +- 0.01	THIS = -0.50 +- 0.01	THIS = -0.22 +- 0.01
SECG = -2.79 +- 0.12	SECG = -3.34 +- 0.12	SECG = -3.30 +- 0.18
THIG = 0.90 +- 0.05	THIG = 0.94 +- 0.05	THIG = 1.09 +- 0.09
Mv = 4.00 +- 3.33 (edge)	Mv = 4.00 +- 3.54 (e)	Mv = 4.00 +- 3.58 (e)
rv = 0.62 +- 0.06	rv = 1.07 +- 0.04	rv = 1.03 +- 0.04
bv = 0.40 +- 0.67	bv = 0.40 +- 0.02 (e)	bv = 0.40 +- 0.03 (e)
C = 8.78 +- 0.98	C = 1.05 +- 0.30	C = 1.23 +- 0.33
MC = 0.97 +- 0.11	MC = 4.00 +- 3.38 (e)	MC = 4.00 +- 3.36 (e)
tMv = 0.88 +- 0.24	tMv = 1.32 +- 2.26	tMv = 1.03 +- 0.82
trv = 7.76 +- 1.39	trv = 0.82 +- 0.19	trv = 0.92 +- 0.23
tbv = 2.05 +- 0.40	tbv = 0.40 +- 0.16 (e)	tbv = 0.40 +- 0.33 (e)
rpi = 3.54 +- 1.77	rpi = 3.38 +- 0.16	rpi = 3.38 +- 0.17
Mpi = 0.73 +- 0.37	Mpi = 4.00 +- 2.33 (e)	Mpi = 4.00 +- 2.35 (e)

- Partial  $\chi^2/npts$

H1ZEUS:	81.74/107	91.64/107	84.11/107
allUNP:	50.20/68	86.11/68	69.10/54 (cut)
CLAS:	116.16/22	68.92/22	58.87/15 (cut)
CLASDM:	18.51/12	11.16/12	8.48/8 (cut)
BSDw:	9.76/12	22.54/12	12.31/8 (cut)
BSSw:	4.13/8	21.39/8	19.58/8
TSA1:	608.33/12	18.66/12	15.62/10 (cut)

## HERMES TSA



# Mellin-Barnes representation of CFFs (I)

- Factorization formula for CFFs ...

$${}^S\mathcal{H}(\xi, \Delta^2, Q^2) = \int dx \mathbf{C}(x, \xi, Q^2/\mu^2) \mathbf{H}(x, \xi, \Delta^2, \mu^2)$$

- ... is in moment space written as **conformal operator product expansion** (COPE)

$${}^S\mathcal{H}(\xi, \Delta^2, Q^2) = 2 \sum_{j=0}^{\infty} \xi^{-j-1} \mathbf{C}_j(Q^2/\mu^2, \alpha_s(\mu)) \mathbf{H}_j(\xi, \Delta^2, \mu^2)$$

## Mellin-Barnes representation of CFFs (I)

- Factorization formula for CFFs ...

$${}^S\mathcal{H}(\xi, \Delta^2, Q^2) = \int dx \mathbf{C}(x, \xi, Q^2/\mu^2) \mathbf{H}(x, \xi, \Delta^2, \mu^2)$$

- ... is in moment space written as **conformal operator product expansion** (COPE)

$${}^S\mathcal{H}(\xi, \Delta^2, Q^2) = 2 \sum_{j=0}^{\infty} \xi^{-j-1} \mathbf{C}_j(Q^2/\mu^2, \alpha_s(\mu)) \mathbf{H}_j(\xi, \Delta^2, \mu^2)$$

- However, this series converges only for unphysical  $\xi > 1$

## Mellin-Barnes representation of CFFs (I)

- Factorization formula for CFFs ...

$${}^S\mathcal{H}(\xi, \Delta^2, Q^2) = \int dx \mathbf{C}(x, \xi, Q^2/\mu^2) \mathbf{H}(x, \xi, \Delta^2, \mu^2)$$

- ... is in moment space written as **conformal operator product expansion** (COPE)

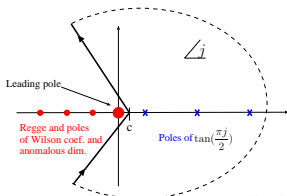
$${}^S\mathcal{H}(\xi, \Delta^2, Q^2) = 2 \sum_{j=0}^{\infty} \xi^{-j-1} \mathbf{C}_j(Q^2/\mu^2, \alpha_s(\mu)) \mathbf{H}_j(\xi, \Delta^2, \mu^2)$$

- However, this series converges only for unphysical  $\xi > 1$
- To evaluate it for  $\xi < 1$  we analytically continue in complex  $j$  plane and write the COPE sum as a **Mellin-Barnes** integral ...

## Mellin-Barnes representation of CFFs (II)

- ... using Sommerfeld-Watson transformation and dispersion relations:

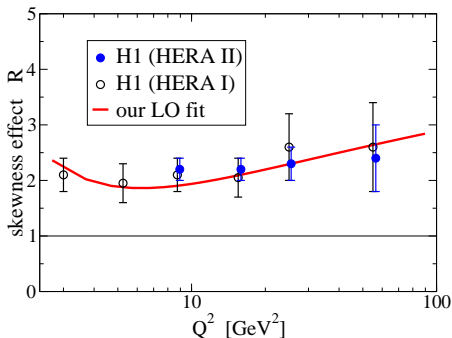
$$\begin{aligned}
 \mathcal{S}\mathcal{H}(\xi, \Delta^2, Q^2) &= 2 \sum_{j=0}^{\infty} \xi^{-j-1} \mathbf{C}_j(Q^2/\mu^2, \alpha_s(\mu)) \mathbf{H}_j(\eta, \Delta^2, \mu^2) \\
 &= \frac{1}{2i} \int_{c-i\infty}^{c+i\infty} dj \xi^{-j-1} \left[ i + \tan\left(\frac{\pi j}{2}\right) \right] \mathbf{C}_j(Q^2/\mu^2, \alpha_s(\mu)) \mathbf{H}_j(\xi, \Delta^2, \mu^2)
 \end{aligned}$$



## Skewness ratio — R

- ... is discriminating feature of GPD models

$$R \equiv \frac{\mathcal{I}m A_{\text{DVCS}}}{\mathcal{I}m A_{\text{DIS}}} \Big|_{t=0} \sim \frac{\sqrt{\sigma_{\text{DVCS}}}}{\sigma_{\text{DIS}}} \stackrel{\text{LO}}{\sim} \frac{H(x, x)}{q(\frac{2x}{1+x}, 0)}$$

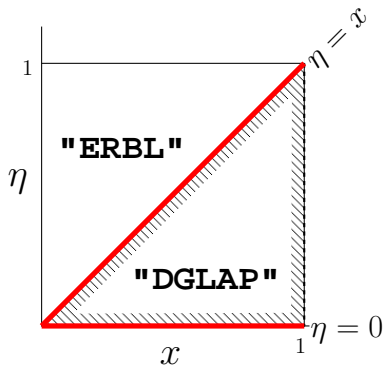


- measurement:  $R \approx 2$

## Skewness ratio (II) — $r$

- Skewness ratio is naturally defined by ratio of GPDs  $H(x, \eta)$  at two physically relevant trajectories:  $\eta = x$  and  $\eta = 0$

$$r = \frac{H(x, x)}{H(x, 0)}$$

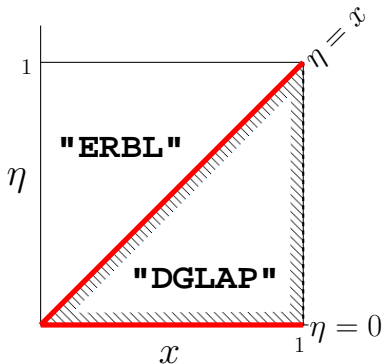




## Skewness ratio (II) — $r$

- Skewness ratio is naturally defined by ratio of GPDs  $H(x, \eta)$  at two physically relevant trajectories:  $\eta = x$  and  $\eta = 0$

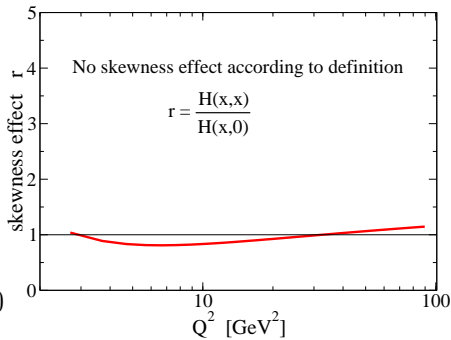
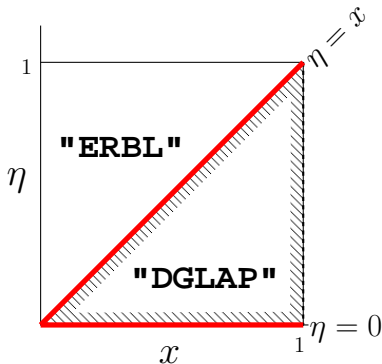
$$r = \frac{H(x, x)}{H(x, 0)} \stackrel{LO}{\approx} \frac{1}{2^\alpha} R \quad \text{for } q(x \rightarrow 0) \sim x^{-\alpha} \quad \alpha \approx 1$$



## Skewness ratio (II) — $r$

- Skewness ratio is naturally defined by ratio of GPDs  $H(x, \eta)$  at two physically relevant trajectories:  $\eta = x$  and  $\eta = 0$

$$r = \frac{H(x, x)}{H(x, 0)} \stackrel{LO}{\approx} \frac{1}{2^\alpha} R \quad \text{for} \quad q(x \rightarrow 0) \sim x^{-\alpha} \quad \alpha \approx 1$$



## Skewness ratio (III)

- Simple GPD models are usually constrained by “natural” DVCS-to-DIS enhancement factor

[Shuvaev et al. '99]

$$r = \frac{2^{j+2}\Gamma(j + 5/2)}{\sqrt{\pi}\Gamma(j + 3)} \Big|_{j=\alpha-1 \approx 0.2} \approx 1.5$$

- ... and thus fail to reproduce data
- Having correct  $r \approx 1$  skewness ratio is an important feature of models that aim to reproduce data at LO.